Published in final edited form as:

Miao, H., Schmidt, J., Heil, T., Antonietti, M., Willinger, M. G., & Guterman, R. (2018). Formation and Properties of Poly(Ionic Liquid)-Carbene Nanogels Containing Individually Stabilized Silver Species. Chemistry – A European Journal, 24(22), 5754-5759. doi:10.1002/chem.201800448.

Formation and Properties of Poly(Ionic Liquid)-Carbene Nanogels Containing Individually Stabilized Silver Species

Han Miao, Johannes Schmidt, Tobias Heil, Markus Antonietti, Marc Willinger, Ryan Guterman

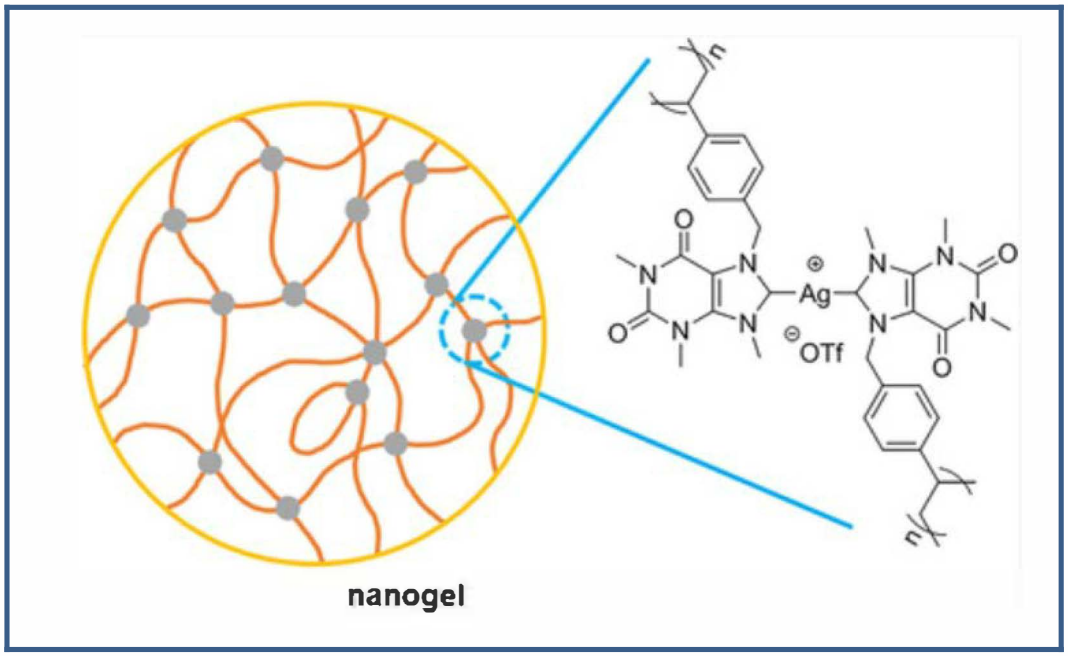

Hierarchical nanostructures: Theophylline-derived poly(ionic liquids) were cross-linked by silver–carbene cross-linking to create nanogels with controllable properties and shape, including small nanogels and large “galaxy-like” super structures (see figure).

Formation and Properties of Poly(Ionic Liquid)-Carbene Nanogels Containing Individually Stabilized Silver Species

Han Miao,[a] Johannes Schmidt,[b] Tobias Heil,[a] Markus Antonietti,[a] Marc Willinger,[a] and Ryan Guterman*[a]

Abstract: Imidazolium-based ionic liquids have the ability to undergo a variety of chemical reactions through an *N*-heterocyclic carbene (NHC) intermediate, which has expanded the chemical toolbox for new applications. Despite their uses and exploration, the carbene-forming properties and applications of their polymeric congeners, poly(ionic liquid)s (PILs), is still underdeveloped. In this work we explore the NHC-forming properties of a theophylline-derived PIL for nanogel synthesis. Using silver oxide as both the carbene forming reagent and crosslinker, nanogels containing individually stabilized ions can be created with different sizes and morphology, including large "galaxy-like" superstructures. Using high-resolution TEM techniques, we directly observed the sub-nanometer structure of these constructs. This features combined exemplifies the unique chemistry of poly-NHCs for single metal ion stabilization nanogel design.

The marriage between NHC and ionic liquid chemistry[1] has expanded the chemical toolbox for new applications, including organic transformations,[2] CO_2 capture,[3] catalysis,[4] and some others.[5] In these reported examples, the properties of imidazolium salts and their carbene forming properties were simultaneously harnessed. For material science applications, it is beneficial to transfer these approaches to polymeric systems such as poly(ionic liquids) (PILs), as they provide greater mechanical stability, ease of handling and processing, and the ability to design macromolecular architectures to fine tune their use.[5b, 6] In a similar sense, transferring small-molecule NHC chemistry to their polymer counterparts is also a key step towards their exploitation, including the attachment of small molecules,[7] metal species,[8] main group elements,[9] and CO_2 capture.[10] The ongoing effort to create super-effective CO_2 separation membranes[11] from imidazolium polymers is a model example for poly-NHCs[10c] with great promise.

One commonality between NHCs and PILs is their ability to disperse/stabilize metallic particles/atoms. Owing to the strong carbon-metal bond of NHCs,[12] it was demonstrated that self-assembled monolayers of NHCs on gold display significantly greater thermal and chemical stability compared to thiols. Meanwhile the strong surface-activating properties of PILs[13] have resulted in their use as powerful dispersing and stabilizing agents for the development of better graphene-based sensors,[14] cathode binders,[15] and metal nanoparticles.[16] Previously we demonstrated that the carbene-forming properties of triazolium-based PILs helps to produce highly dispersed, catalytically active metal clusters and hints towards the significant role PIL-NHC hybrids have in their fabrication.[17] Despite these investigations, there are no comprehensive reports outlining the synthesis and structure of PIL-NHC hybrid materials. Through the combined effects of the PIL and NHCs, greater levels of stability/chelation on both the atomic and nanometer scales may be achieved for the development of high-performing and reusable catalysts. Such is the case for the iron-based catalyst by Driess *et al.*,[18] where the chelating NHC ligand allows for the unusually high stabilization and synthesis of an η^6-arene iron(0) complex for the catalytic reduction of amines. Previously we have demonstrated that the hydrogen evolution reaction is enhanced when using atomically-dispersed silver in a carbon-nitride matrix and further illustrates the need for designing new, single-atom stabilized systems.[19]

In the present paper, we explore an approach to evenly disperse covalently bound silver ions within a PIL/NHC nanogel though silver-carbene crosslinking. Using a theophylline-derived PIL rather than a small-molecule for NHC formation,[20] the polymer chains become crosslinked through a silver bridge which simultaneously constitute the self-stabilized metal/NHC/PIL nanogels. The crosslinking step promotes the formation of surprisingly well-defined, spherical nanogels whose size and physical properties could be tuned depending on the reaction conditions. The internal structure of these materials was elucidated using high-resolution TEM and XPS, showing for the first time individually stabilized silver ions within such a polymer matrix, providing direct evidence for the effectiveness of this approach for metal stabilization. Core/shell structures of the silver nanoparticle/PIL-NHC hybrid were also observed and provides insight into the formation mechanism of these unique materials.

The theophylline derived polymer was synthesized according to a literature procedure.[20] Briefly, theophylline was combined with 4-vinylbenzyl chloride and NaH in DMSO to attach the polymerizable group, followed by quaternization using MeOTf, and free-radical polymerization to create the final polymer (Figure 1). Our choice for using theophylline as our substrate was motivated by its biological origin, but also by its known carbene chemistry,[21] creating rather stable silver carbenes under ambient conditions. This provides entry to a more green synthetic approach for such cationic polyelectrolytes and poly-NHCs. Ag_2O acts not only as a silver source, but also as a base which deprotonates the imidazolium.[12f, 22] The resulting Ag-NHC bond that is formed is a result of the strong σ-donor character of the NHC lone pair with some backbonding contribution from the silver atom.[23]

[a] Dr. H. Miao, Dr. T. Heil, Prof. Dr. M. Antoniette, Dr. M. Willinger, Dr. R. Guterman
Department of Colloid Chemistry
Max Planck Institute for Colloids and Interfaces
Am Mühlenberg 1, MPI Research Campus Golm, 14476 Potsdam (Germany)
E-mail: Ryan.Guterman@mpikg.mpg.de

[b] Dr. J. Schmidt
Department of Functional Materials
Technical University Berlin
Hardenbergstr. 40, 10623 Berlin (Germany)

Supporting information for this article is given via a link at the end of the document.

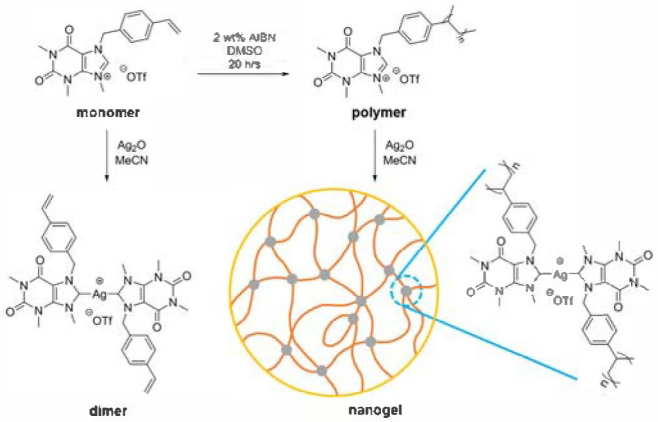

Figure 1. Synthesis of Ag-NHCs from the theophylline-derived monomer to form a dimer, and from the theophylline-derived poly(ionic liquid) to create crosslinked silver/NHC/PIL.

Computational studies conducted by Meyer and Frenking et. al determined that σ-donation to the metal center is dominant, but not exclusive.[24] For a variety of group 11 metal NHC complexes, metal-NHC π-backbonding interactions contribute a small amount (~15-30%) of the complexs' orbital interaction energies, with variation depending on the metal. They found that copper tended to undergo greater, π-backbonding with respect to both Au and Ag.[24a] With regards to the NHC structure, π-backbonding contributions are increased by the use of highly conjugated NHCs, such as those derived from caffeine.[25] The overall lower contribution of π-backbonding from the metal in NHC complexes is in part a result of significant π-donation from the nitrogen atoms in to the empty p_y-orbital (also referred to as p_π, the out-of-plane orbital) of the carbene. In the case of Ag^+, σ-donation from the NHC is to the empty 5s orbital, while π-backbonding proceeds from a filled 4d orbital to p_π.[26] Depending on the anion, a variety of bonding motifs have been observed,[12f, 27] including dimers when non-coordinating anions (OTf^-, BF_4^-, PF_6^-) are present.[28] Given the triflate anion in the monomer, we would expect the formation of a dimer similar to reported compounds (Figure 1, left).[29] Upon treatment of the monomer with excess Ag_2O in MeCN (24 hr), we observed a decrease in the intensity of the C8 proton (RN(*CH*)NR, δ = 9.44) and an upfield shift for the aryl protons (δ = 7.50-7.20). Integration of the C8 proton relative to the olefin and methyl signals (δ = 6.67 and 4.16 respectively) revealed that the reaction proceeded for the monomer nearly to completion (95%), and that the polymerizable groups remained intact with no other byproducts (Figure S1). The reaction was also carried out in deuterated acetonitrile to examine whether a stable acetonitrile complex was formed as a major product (Figure S2). In such case, we would expect a strong resonance at δ = ~2.0, however there is little evidence for its formation as a major or stable product. This is also accompanied by the appearance of a resonance at δ = 187.8 in the $^{13}C\{^1H\}$ NMR spectrum which is attributed to the Ag-*C* carbon, consistent with the formation of other caffeine-derived Ag-NHC dimers (Figure S3 top and S4, top).[29b] Work by Hahn *et. al* also shows that the dimer product is likely to form in acetonitrile solutions by harnessing the dimer structure for a [2+2] cyclization, which can only occur in the dimerized Ag-NHC complex.[30] Mass spectrometry analysis of the compound further confirms the presence of the dimer with the isotope distribution consistent with calculated spectra (Figure S5 and S6). While this dimer was not stable (silver precipitate was observed after 24 hr), this does confirm these theophylline-derived units may undergo dimerization. The lack of stability may be a result of insufficient steric protection at the nitrogen positions or the presence of reactive/autopolmyerizable alkene groups that can reduce silver, which in the latter would be eliminated in the PIL.[31] We then treated the PIL with Ag_2O using a variety of conditions, including different stoichiometry and concentrations to determine silver uptake and properties (Table 1). After stirring for 5 hr, the solutions were filtered, solvent removed *in vacuo*, and an off-white powder was isolated for **A-C** and a slightly purple powder for **D**. This material did not change color when in storage, unlike the dimer. Analysis of **D** by ^1H-NMR spectroscopy (Figure S7) revealed significant broadening of the signals after reaction with silver, and the retention of some of the C8 proton after reaction. Broadening of the resonances is indicative of crosslinking and/or aggregation of polymers resulting from an increase in restricted mobility of the polymer. Longer reaction times between the PIL and Ag_2O resulted in complete disappearance of the C8 proton signal and even greater broadening (Figure S8). Like in the dimer, this is also accompanied by the appearance of a resonance at δ = 187.3 (Ag-*C*) in the $^{13}C\{^1H\}$ NMR spectrum providing direct evidence for the formation of the Ag-NHC in the PIL (Figure S3 bottom and S4 bottom). While it is possible that dissolved silver ions may aggregate the PIL through interactions between the nitrogen atoms and/or alkenes present in the PIL, we found that the addition of AgOTf, a silver reagent that cannot promote the formation of an NHC, does not result in any broadening of the resonances in the ^1H NMR spectrum (Figure S9). This control experiment provides supporting evidence that the observed broadening of the PIL upon Ag_2O treatment is primarily a result of Ag-NHC crosslinking and the chemistry thereafter, and to a lesser degree, aggregation/flocculation of the PIL by dissolved silver ions. Furthermore, the formation of an NHC between a PIL and metal is supported by the recent work of Yuan *et. al* where PILs containing both nitrogen atoms and alkenes undergo NHC formation.[17] Analysis using energy-dispersive X-ray spectroscopy (EDX) revealed that silver uptake increased with higher concentrations and added Ag_2O, ranging from 0.8 to 9.1 wt% (Table 1), and that an even distribution of silver through the polymer was present (Figure S10). In this silver content range, a combination of NHCs and the native cationic monomer units should remain. This is observed in the ^1H NMR spectrum (Figure S7), thus supporting forming the silver/NHC/PIL hybrid nanogel (Figure 1, right).

To further understand the silver/NHC/PIL nanogel structure, we measured the averaged hydrodynamic radius $\langle R_H \rangle$ and averaged gyration radius $\langle R_G \rangle$ by DLS and SLS, which provides information related to these materials in solution (Table 1). From **A** to **C**, both the averaged hydrodynamic radius $\langle R_H \rangle$ and averaged gyration radius $\langle R_G \rangle$ became smaller, indicating that increased crosslinking occurred with greater silver incorporation. **D** in contrast displayed very high values, which indicates that higher concentrations facilitate greater interpolymeric

crosslinking and/or aggregation between the PIL chains. The larger ρ-ratio for **A**-**C** indicates that the polymer chains inside the particle are very loose and possess an extended morphology, however the decreasing ρ-ratio from **A** to

Table 1. The effect of reaction conditions on the silver content for nanogels **A**-**D**.

Sample[a]	Concentration (mg/mL)	Silver oxide (mg/mL)	Ag content (wt %)	$\langle R_H \rangle$ [b] (nm)	$\langle R_G \rangle$ [c] (nm)	ρ-ratio ($\langle R_G \rangle / \langle R_H \rangle$)
A	10.0	0.84	0.84±0.1	21.4	47.5	2.22
B	10.0	1.6	2.5±0.6	20.2	32.9	1.63
C	10.0	2.4	5.8±1.1	19.9	24.7	1.24
D	10.0	1.6	9.1±0.6	62.8	59.1	0.94

[a] 25 mg of polymer was used for sample preparation. [b] $\langle R_H \rangle$ average hydrodynamic radius (measured by dynamic light scattering). [c] $\langle R_G \rangle$ average gyration radius (by static light scattering).

C indicates that the particle is becoming more compact. This can be explained by an increase in intrapolymeric crosslinking reactions between silver and polymer within the nanogel, resulting in the formation of more spherical crosslinked particles. Given the over 7-fold increase in silver content from **A**-**C** (0.84 to 5.8 wt%), higher degrees of crosslinking between polymer chains is expected. For sample **D**, we observed a significant increase in both $\langle R_H \rangle$ and $\langle R_G \rangle$, however the ρ-ratio was lowest of all at 0.94, indicating the formation of large, dense materials. While performing the reaction at a higher concentration promotes interpolymeric crosslinking reactions, internanogel crosslinking should also be promoted, and create larger structures with a more localized, dense architecture. As supporting evidence, we measured the sedimentation behavior of these materials (Figure S11). We found that from the pure polymer to sample **D**, the sedimentation coefficient increased, indicating that the produced materials are becoming denser and/or larger, thus supporting these data.

The indirect probing method of light scattering techniques begs the question of the true nature and fine structure of these nanogels. Using high-resolution TEM, we examined samples **A**-**D** and found that the internal structures of the nanogels vary. In all cases, we clearly observed well-defined, individual silver species throughout the silver/NHC/PIL nanogel structures (Figure 2). For **A**-**C**, the silver is evenly dispersed within the nanogels in a random fashion, and in very close proximity to each other, with nanogels in **A** (Figure 2a and Figure S12) appearing to be more diffuse than **B** or **C** (Figure 2b, Figure S13 and Figure 2c, Figure S10). In contrast to this, **D** displayed completely different features with large, "galaxy-like", hierarchical superstructures of ~150 nm in diameter, possessing a dense center ~50 nm in size (Figure 2d and Figure S15). Magnification of the periphery revealed particles possessing a core-shell type structure (Figure 2e), where the core appears to contain crystallized silver atoms surrounded by a halo of silver/NHC/PIL material of similar quality to what is observed in **B** and **C**. Figure 2f shows the atomic structure of one of the crystalline cores. The hexagonal arrangement of the atomic columns and the lattice spacing of 0.23 ± 0.02 nm, measured utilizing Fourier transformation of a crystalline core region, matches well with the theoretical value of 0.2361 nm for the face centered cubic structure of Ag^0 when observed along the (111) plane.[32] To identify the different silver species in the XPS spectra we analyzed expected single components (Ag_2O, $AgCF_3SO_3$ and the Ag-NHC dimer) for their peak positions. With the data of these species it was not possible to achieve an acceptable fit for the respective measured XPS spectra. Therefore we added a 4th peak (Ag $3d_{5/2}$ 368.47 eV; Ag $3d_{3/2}$ 374.46 eV) and with these 4 peaks we obtained fits with high Abbe criterions for all spectra with the same peak positions. The peak for Ag^0 is expected for 368.2 eV,[33] but it was shown before, that for small metal particles and cluster the binding energies in XPS analysis are shifted to higher eV compared to the bulk metal.[34] Therefore we believe that this peak belongs to Ag^0 and assigned the peak accordingly (Table S1, S2, and Figure S16-S19). The TEM images, XPS data, and the strong color and broad UV-vis spectral features (Figure S20) observed for **D** support the presence of metallic silver nanoparticles of broad size distribution and/or aggregation. The mechanism of formation for the observed nanogels here may be explained by several contributing factors. On one hand, we showed earlier that crosslinking between PIL chains by Ag-NHCs explains, in part, how the PIL chains may aggregate. However, the presence of silver nanoparticles within solution and their interactions with the PIL (crosslinked or not) should also result in aggregation/flocculation processes by adsorption of PIL on to the surface of these nanoparticles. This model has been demonstrated by Cabane, where polymer can adsorb on to particle surfaces resulting in aggregation.[35] While it is not possible to say here which of these two processes dominate, the observed structures are likely a combination of these two effects. XPS results show that a decrease in the amount of Ag-NHC in the polymer is accompanied by an increase in the amount of Ag^0, indicating that perhaps silver from the Ag-NHC complex convert to Ag^0; although this evidence is not conclusive. Silver particles that do form would also preferentially adsorb silver ions from solution (either as AgOTf or from the Ag-NHC) and undergo further growth. With these two mechanisms in mind, we propose a model for the creation of the observed structures (Figure 2g). In the first stages, the PILs are crosslinked by the formation of Ag-NHC complexes between the chains to form nanogels. Silver nanoparticles formed either from 1) the Ag-NHC within the crosslinked polymer, or 2) from dissolved silver ions in solution, are then adsorbed by the PIL. These silver nanoparticles undergo growth by incorporating silver either from the Ag-NHCs or by adsorbing dissolved silver ions on to its surface. Such structures then grow by a combination of Ag-NHC crosslinking and aggregation/flocculation to create large structures observed here. Aggregation of the silver nanoparticles in **D** appears to be greater, with a strong, broad absorbance at 425 nm in the UV-vis spectrum, typical of metallic silver nanoparticles (Figure S20). Meanwhile a weaker absorbance was noticed for **A**-**C**, indicating that this process is not dominant in the latter.[32, 36] While the exact reduction mechanism is not known here, silver ions do oxidize a variety organic molecules such as acetone and DMF, among others to varying degrees.[37]

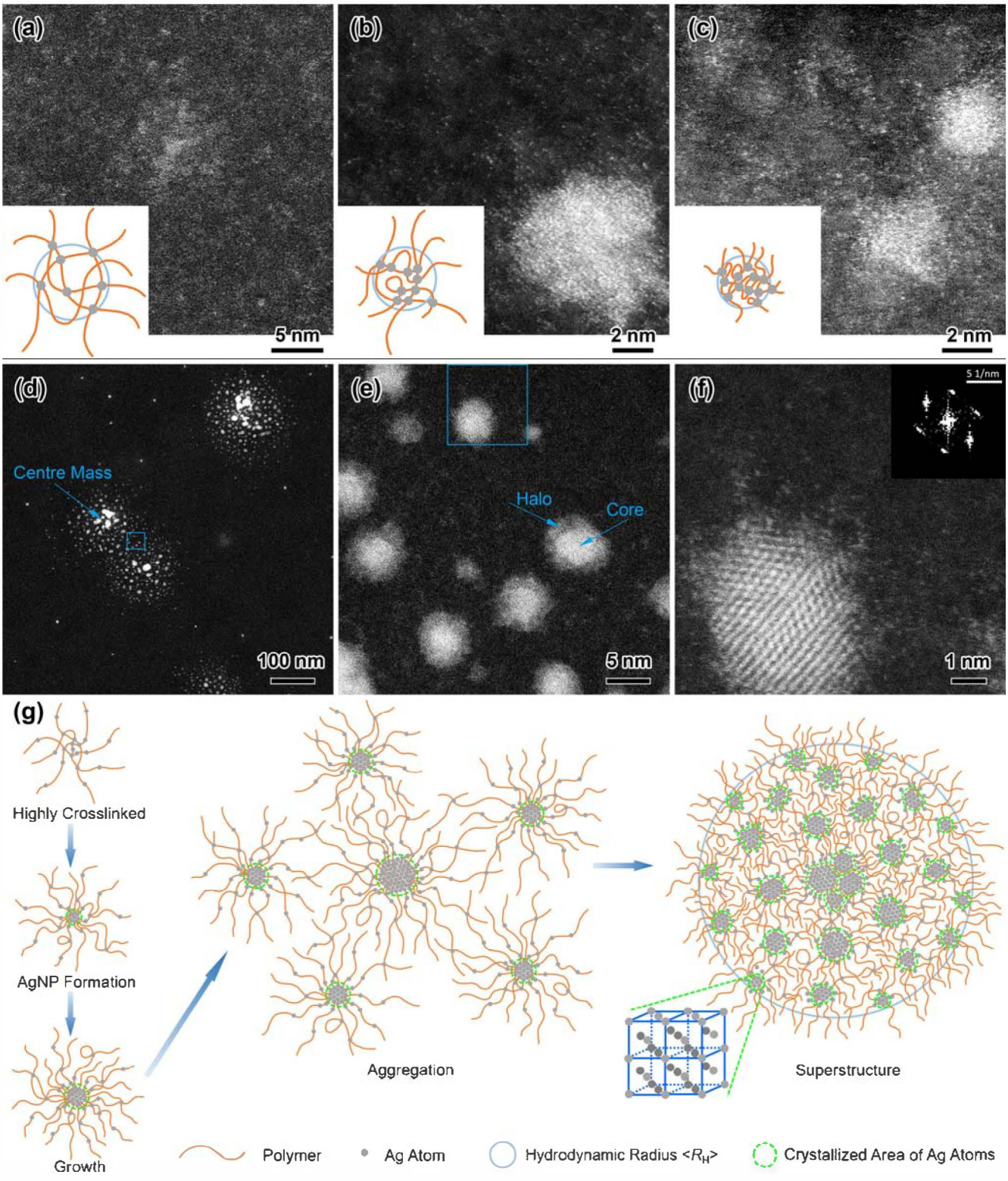

Figure 2. High-resolution STEM images of the nanogels: (a) sample **A**, (b) sample **B**, (c) sample **C**, and (d) sample **D**. The insets show the morphology of each sample. The silver atoms in the background are likely a mixture of free silver/NHC/PIL material, or AgOTf, a byproduct from the reaction. (e) Magnification of the blue square in (d), haloed silver particles. (f) Magnification of the blue square in (e), crystallized core of the haloed silver particles. Inset: Fourier transformation of the crystallized core. (g) Aggregation mechanism of the "galaxy-like" superstructure observed sample **D** by PIL adsorption on silver nanoparticles and NHC crosslinking.

In conclusion, a theophylline-derived PIL was reacted with silver oxide to form stabilized nanogels through a carbene crosslinking reaction. These silver/NHC/PIL nanogels were colloidally stable and capable of covalently immobilizing single silver ions within its structure. Systematic changes in the nanogel topology using DLS, SLS and AUC were found, from loosely to highly crosslinked silver/NHC/PIL hybrids, to large superstructures containing silver nanoparticles. The formation of these structures is a result of both Ag-NHC crosslinking and aggregation by PIL on the surface of the silver nanoparticles, with structural variations depending on initial reaction parameters. At high silver loading, hierarchical nanostructures were observed containing metallic silver particles comprised of a dense center-mass. These observations demonstrated the dynamic behavior of these systems and the unique behavior of combining NHC with PIL chemistry. To our knowledge, this is the first example where the density of silver ions within a confined space can be related to the cluster/nanoparticle forming properties. Furthermore the ability to create stable colloids containing highly immobilized single metal ions, such as silver which can be used as a transmetallation reagent, will be of interest for catalysis application where both high stability and accessibility is required.

Experimental Section

All experimental details are compiled in the Supporting Information.

Acknowledgements

The authors would like to acknowledge Antje Voelkel for performing and analyzing the AUC experiments, and Technische Universität Berlin for access to their XPS facility.

Keywords: poly(ionic liquid)s • *N*-heterocyclic carbene • nanogel • hierarchical nanostructure • crosslinking density

[1] M. Fèvre, J. Pinaud, Y. Gnanou, J. Vignolle, D. Taton, *Chem. Soc. Rev.* **2013**, *42*, 2142-2172.

[2] a) V. K. Aggarwal, I. Emme, A. Mereu, *Chem. Commun.* **2002**, 1612-1613; b) G. Forte, I. Chiarotto, A. Inesi, M. A. Loreto, M. Feroci, *Adv. Synth. Catal.* **2014**, *356*, 1773-1781; c) E. A. B. Kantchev, C. J. O'Brien, M. G. Organ, *Angew. Chem. Int. Ed.* **2007**, *46*, 2768-2813; d) D. W. Morrison, D. C. Forbes, J. H. Davis, *Tetrahedron Lett.* **2001**, *42*, 6053-6055.

[3] a) O. Hollóczki, D. S. Firaha, J. Friedrich, M. Brehm, R. Cybik, M. Wild, A. Stark, B. Kirchner, *J. Phys. Chem. B* **2013**, *117*, 5898-5907; b) H. Peng, Y. Zhou, J. Liu, H. Zhang, C. Xia, X. Zhou, *RSC Adv.* **2013**, *3*, 6859-6864; c) F. Yan, M. Lartey, K. Damodaran, E. Albenze, R. L. Thompson, J. Kim, M. Haranczyk, H. B. Nulwala, D. R. Luebke, B. Smit, *PCCP* **2013**, *15*, 3264-3272.

[4] a) D. Enders, O. Niemeier, A. Henseler, *Chem. Rev.* **2007**, *107*, 5606-5655; b) J. D. Scholten, J. Dupont, *Organometallics* **2008**, *27*, 4439-4442; c) L. Xu, W. Chen, J. Xiao, *Organometallics* **2000**, *19*, 1123-1127.

[5] a) A. Piermattei, S. Karthikeyan, R. P. Sijbesma, *Nat. Chem.* **2009**, *1*, 133-137; b) J. Raynaud, N. Liu, M. Fèvre, Y. Gnanou, D. Taton, *Polym. Chem.* **2011**, *2*, 1706-1712; c) B. R. Van Ausdall, J. L. Glass, K. M. Wiggins, A. M. Aarif, J. Louie, *J. Org. Chem.* **2009**, *74*, 7935-7942.

[6] a) L. C. Tomé, M. Isik, C. S. Freire, D. Mecerreyes, I. M. Marrucho, *J. Memb. Sci.* **2015**, *483*, 155-165; b) J. Yuan, M. Antonietti, *Polymer* **2011**, *52*, 1469-1482; c) P. Zhang, J. Yuan, T. P. Fellinger, M. Antonietti, H. Li, Y. Wang, *Angew. Chem. Int. Ed.* **2013**, *52*, 6028-6032.

[7] a) M. Rose, A. Notzon, M. Heitbaum, G. Nickerl, S. Paasch, E. Brunner, F. Glorius, S. Kaskel, *Chem. Commun.* **2011**, *47*, 4814-4816; b) J. M. Storey, C. Williamson, *Tetrahedron Lett.* **2005**, *46*, 7337-7339; c) M. Tan, Y. Zhang, J. Y. Ying, *Adv. Synth. Catal.* **2009**, *351*, 1390-1394.

[8] a) A. B. Powell, C. W. Bielawski, A. H. Cowley, *J. Am. Chem. Soc.* **2009**, *131*, 18232-18233; b) W. J. Sommer, M. Weck, *Adv. Synth. Catal.* **2006**, *348*, 2101-2113.

[9] a) M. Asay, C. Jones, M. Driess, *Chem. Rev.* **2010**, *111*, 354-396; b) H. M. Tuononen, R. Roesler, J. L. Dutton, P. J. Ragogna, *Inorg. Chem.* **2007**, *46*, 10693-10706.

[10] a) A. Dani, V. Crocellà, C. Magistris, V. Santoro, J. Yuan, S. Bordiga, *J. Mater. Chem. A* **2017**, *5*, 372-383; b) J. Pinaud, J. Vignolle, Y. Gnanou, D. Taton, *Macromolecules* **2011**, *44*, 1900-1908; c) S. N. Talapaneni, O. Buyukcakir, S. H. Je, S. Srinivasan, Y. Seo, K. Polychronopoulou, A. Coskun, *Chem. Mater.* **2015**, *27*, 6818-6826; d) A. Wilke, J. Yuan, M. Antonietti, J. Weber, *ACS Macro Lett.* **2012**, *1*, 1028-1031.

[11] a) J. E. Bara, E. S. Hatakeyama, D. L. Gin, R. D. Noble, *Polym. Adv. Technol.* **2008**, *19*, 1415-1420; b) W. Fang, Z. Luo, J. Jiang, *PCCP* **2013**, *15*, 651-658.

[12] a) C. M. Crudden, J. H. Horton, I. I. Ebralidze, O. V. Zenkina, A. B. McLean, B. Drevniok, Z. She, H.-B. Kraatz, N. J. Mosey, T. Seki, *Nat. Chem.* **2014**, *6*, 409-414; b) M. N. Hopkinson, C. Richter, M. Schedler, F. Glorius, *Nature* **2014**, *510*, 485-496; c) C. Lee, C. S. Vasam, T. Huang, H. Wang, R. Yang, C. Lee, I. J. Lin, *Organometallics* **2006**, *25*, 3768-3775; d) G. Occhipinti, V. R. Jensen, *Organometallics* **2011**, *30*, 3522-3529; e) J. Vignolle, T. D. Tilley, *Chem. Commun.* **2009**, 7230-7232; f) H. M. Wang, I. J. Lin, *Organometallics* **1998**, *17*, 972-975.

[13] a) K. P. Charan, N. Pothanagandhi, K. Vijayakrishna, A. Sivaramakrishna, D. Mecerreyes, B. Sreedhar, *Eur. Polym. J.* **2014**, *60*, 114-122; b) K. Grygiel, B. Wicklein, Q. Zhao, M. Eder, T. Pettersson, L. Bergström, M. Antonietti, J. Yuan, *Chem. Commun.* **2014**, *50*, 12486-12489; c) M. Tokuda, T. Shindo, H. Minami, *Langmuir* **2013**, *29*, 11284-11289.

[14] a) H. Mao, J. Liang, H. Zhang, Q. Pei, D. Liu, S. Wu, Y. Zhang, X.-M. Song, *Biosens. Bioelectron.* **2015**, *70*, 289-298; b) T. T. Tung, M. Castro, T. Y. Kim, K. S. Suh, J.F. Feller, *Anal. Bioanal. Chem.* **2014**, *406*, 3995-4004.

[15] J.-S. Lee, K. Sakaushi, M. Antonietti, J. Yuan, *RSC Adv.* **2015**, *5*, 85517-85522.

[16] K. Manojkumar, A. Sivaramakrishna, K. Vijayakrishna, *J. Nanopart. Res.* **2016**, *18*, 1-22.

[17] J.k. Sun, Z. Kochovski, W.-Y. Zhang, H. Kirmse, Y. Lu, M. Antonietti, J. Yuan, *J. Am. Chem. Soc.* **2017**, *139*, 8971-8976.

[18] B. Blom, G. Tan, S. Enthaler, S. Inoue, J. D. Epping, M. Driess, *J. Am. Chem. Soc.* **2013**, *135*, 18108-18120.

[19] a) Z. Chen, S. Mitchell, E. Vorobyeva, R. K. Leary, R. Hauert, T. Furnival, Q. M. Ramasse, J. M. Thomas, P. A. Midgley, D. Dontsova, *Adv. Funct. Mater.* **2017**, *27*, 1605785; b) Z. Chen, S. Pronkin, T.P. Fellinger, K. Kailasam, G. Vilé, D. Albani, F. Krumeich, R. Leary, J. Barnard, J. M. Thomas, *ACS nano* **2016**, *10*, 3166-3175.

[20] R. Guterman, M. Antonietti, J. Yuan, *Macromol. Rapid Commun.* **2017**, *38*, 1600748.

[21] H. A. Mohamed, B. R. Lake, T. Laing, R. M. Phillips, C. E. Willans, *Dalton Trans.* **2015**, *44*, 7563-7569.

[22] J. M. Hayes, M. Viciano, E. Peris, G. Ujaque, A. Lledós, *Organometallics* **2007**, *26*, 6170-6183.

[23] a) M. W. Hussong, W. T. Hoffmeister, F. Rominger, B. F. Straub, *Angew. Chem. Int. Ed.* **2015**, *54*, 10331-10335; b) D. Marchione, L. Belpassi, G. Bistoni, A. Macchioni, F. Tarantelli, D. Zuccaccia, *Organometallics* **2014**, *33*, 4200-4208.

[24] a) X. Hu, I. Castro-Rodriguez, K. Olsen, K. Meyer, *Organometallics* **2004**, *23*, 755-764; b) D. Nemcsok, K. Wichmann, G. Frenking, *Organometallics* **2004**, *23*, 3640-3646.

[25] J. J. Hu, S.Q. Bai, H. H. Yeh, D. J. Young, Y. Chi, T. A. Hor, *Dalton Trans.* **2011**, *40*, 4402-4406.
[26] A. Munoz-Castro, *The Journal of Physical Chemistry A* **2011**, *116*, 520-525.
[27] a) X. Hu, Y. Tang, P. Gantzel, K. Meyer, *Organometallics* **2003**, *22*, 612-614; b) C. Lee, K. Lee, I. J. Lin, *Organometallics* **2002**, *21*, 10-12.
[28] a) A. J. Arduengo III, H. R. Dias, J. C. Calabrese, F. Davidson, *Organometallics* **1993**, *12*, 3405-3409; b) I. J. Lin, C. S. Vasam, *Coord. Chem. Rev.* **2007**, *251*, 642-670.
[29] a) A. Kascatan-Nebioglu, A. Melaiye, K. Hindi, S. Durmus, M. J. Panzner, L. A. Hogue, R. J. Mallett, C. E. Hovis, M. Coughenour, S. D. Crosby, *J. Med. Chem.* **2006**, *49*, 6811-6818; b) A. Kascatan-Nebioglu, M. J. Panzner, J. C. Garrison, C. A. Tessier, W. J. Youngs, *Organometallics* **2004**, *23*, 1928-1931.
[30] N. Sinha, F. E. Hahn, *Acc. Chem. Res.* **2017**, *50*, 2167-2184.
[31] H. V. Huynh, Y. Han, R. Jothibasu, J. A. Yang, *Organometallics* **2009**, *28*, 5395-5404.
[32] S. Agnihotri, S. Mukherji, S. Mukherji, *RSC Adv.* **2014**, *4*, 3974-3983.
[33] C. D. Wanger, W. M. Riggs, L. E. Davis, J. F. Moulder, G. E.Muilenberg, *Handbook of X-ray Photoelectron Spectroscopy*, Perkin-Elmer Corp., Physical Electronics Division, Eden Prairie, Minnesota, USA, **1979**.
[34] a) I. Lopez-Salido, D. C. Lim, R. Dietsche, N. Bertram, Y. D. Kim, *J. Phys. Chem. B* **2006**, *110*, 1128-1136; b) I. Lopez-Salido, D. C. Lim, Y. D. Kim, *Surf. Sci.* **2005**, *588*, 6-18.
[35] B. Cabane, *The Journal of Physical Chemistry* **1977**, *81*, 1639-1645.
[36] a) D. K. Bhui, H. Bar, P. Sarkar, G. P. Sahoo, S. P. De, A. Misra, *J. Mol. Liq.* **2009**, *145*, 33-37; b) N. R. Jana, T. K. Sau, T. Pal, *J. Phys. Chem. B* **1999**, *103*, 115-121; c) G. Martinez-Castanon, N. Nino-Martinez, F. Martinez-Gutierrez, J. Martinez-Mendoza, F. Ruiz, *J. Nanopart. Res.* **2008**, *10*, 1343-1348.
[37] a) S. Y. Eom, S. L. Ryu, H. L. Kim, C. H. Kwon, *Colloids and Surfaces A: Physicochemical and Engineering Aspects* **2013**, *422*, 39-43; b) L. M. Liz-Marzán, I. Lado-Touriño, *Langmuir* **1996**, *12*, 3585-3589.